EGTRIB Journal

JOURNAL OF
THE EGYPTIAN SOCIETY OF TRIBOLOGY
VOLUME 22, No. 2, April 2025, pp. 61 - 70 ISSN 2090 - 5882
(Received January 05. 2025, Accepted in final form February 08. 2025) jest.journals.ekb.eg

ARM ROTATING SENSOR BASED ON TRIBOELECTRIC NANOGENERATOR

Ali A. S.[1], Zeinab A. H.[2], Al-Kabbany A. M.[2, 3], Ali W. Y.[2] and Rashed A.[2]

[1]Mechanical Engineering Dept., Faculty of Engineering, Suez Canal University, EGYPT,
[2]Department of Production Engineering and Mechanical Design, Faculty of Engineering, Minia University, Minia 61111, EGYPT,
[3]Smart Biomaterials and Bioelectronics Lab, National Taiwan University, TAIWAN.

ABSTRACT
The present work aims to test the performance of the proposed joint motion triboelectric sensor to be applied in rehabilitation treatments to enhance human arm mobility. The function of the proposed sensor is to harvest energy from the human arm rotation to monitor the rehabilitation training of the patients.

The present study revealed that the output voltage of the proposed sensor is proportional to the value of the rotating arm angle, ensuring its suitability and sustainability. Selecting PA/PTFE as friction surfaces showed the highest values compared to PA/PET and PA/Kapton. The highest voltage values were recorded by thin SR reinforced by Al and Cu nets. Based on the experimental results, it is recommended to conduct further experimental work to enhance the efficiency of the proposed sensor.

KEYWORDS
Arm rotating sensor, triboelectrification, rehabilitation, wearable sensors, silicone rubber (SR).

INTRODUCTION
The contact/separation and sliding of two dissimilar materials on each other generate electrostatic charge (ESC). This phenomenon is called triboelectrification, [1, 2]. The mechanism of ESC is electron, ion, and material transfer, [3]. Electron transfer in insulators occurs on their surfaces, [4]. The triboelectric series has been suggested to determine the polarity of ESC generated on the two surfaces, [5, 6]. The upper surface in the triboelectric series will gain positive ESC, while the other will gain negative ESC. It is revealed that strain generates ESC, [7]. because strain increases the number of contacts charged asperities. Strain strongly influences the magnitude of ESC. Due to the alteration of the physical and chemical properties of the surface. Added to that, strain produces ions and electrons.

A finger-wearable sensor was developed to record the flexion-extension of finger joint by observing the positive and negative voltage output generated from the slip of the two electrification surfaces, [8]. Triboelectrification is used to harvest energy from human movement and convert into electric current. A stretchable structure consisted of silicone rubber and silver-coated glass microspheres, [9]. It was proven that the device was tested for wearable energy harvesting. It can be fixed on different parts of body to harvest energy generated from human motion. Triboelectric nanogenerator made of textiles was proposed in wearable clothes. It consisted of silicone rubber as the negative surface as well as conductive thread working as the electrode, [10]. The output signal was generated from the contact and separation between silicone rubber and human skin.

Triboelectrification is used to harvest energy from human movement and convert into electric current. A stretchable structure consisted of silicone rubber and silver-coated glass microspheres, [11]. It was proven that the device was tested for wearable energy harvesting. It can be fixed on different parts of body to harvest energy generated from human motion. A triboelectric nanogenerator made of textiles was proposed in wearable clothes. It consisted of silicone rubber as the negative surface as well as conductive thread working as the electrode, [12]. The output signal was generated from the contact and separation between silicone rubber and human skin.

The disability and death are caused by the incidence of stroke, [13]. Activities of arm and hand are influenced for many stroke patients, [14 - 16]. Stroke or cerebrovascular disease (CVA) is characterized by interruption of the cerebral circulation at any part by occlusion or rupture of blood vessels. Stroke is the main reason of disabilities, [17 - 19]. The spasticity of the arm results from the increase in tonic stretch reflexes and muscle tone, [20, 21].

It is necessary to treat muscle weakness to avoid muscle atrophy and disability of hand function. Hand spasticity is characterized by flexion of the elbow and rotation of the shoulder, [22]. It is known that mobilization and spasticity cause musculoskeletal tightness that decreases the arm recovery, [23], where spasticity is accompanied by pain, contracture, fibrosis, and weakness of muscles.

In the present work, it is aimed to design a sensor depends on the triboelectrification to detect the rotating motion of the arm during rehabilitation treatment.

EXPERIMENTAL

The sensor proposed in the present work is a triboelectric nanogenerator that consists of two surfaces, which are oppositely charged, as well as an electrode that generates external output. The proposed sensor was constructed to feel the ESC generated from the slip of the contacting materials, resulting from the flexion and extension of the arm. Four types of sensors were examined in the present work. The first sensor consisted of polyamide (PA) textile of 25 µm thickness as the first electrification surface, contacting Kapton, polyester (PET), and polytetrafluorethylene (PTFE) of the same thickness, representing the opposite electrification surface. The two

electrodes were made of a copper sheet of 25 µm thickness stuck to the contacting surfaces, Fig. 1. The second sensor consisted of silicone rubber (SR) as the negative surface and PA surface as the positive one, as well as a copper strip as two electrodes, Fig. 2. While in the third sensor, Fig. 3, SR was reinforced by a copper wire of 0.25 mm diameter. The super elasticity of SR enabled the slip between copper wires and SR matrix during deformation to produce an electric current, resulting from the friction between copper wires and SR. The fourth sensor replaced the copper wire by net of aluminum and copper, Fig. 4. The terminals of the measured voltage were the wire and the earth in the third and fourth sensors. The sensor was fixed in the joint of the arm by sticker. The sensor performance was tested at 45, 90, 135, and 180° rotating angle of arm, Fig. 5. The function of the sensor depends on the idea that the relative displacement of the two contacting electrification surfaces at the joint during rotation is proportional to the rotating angle. Every experiment includes five angular movements, where the pulses of the output voltage of positive/negative were recorded by Arduino.

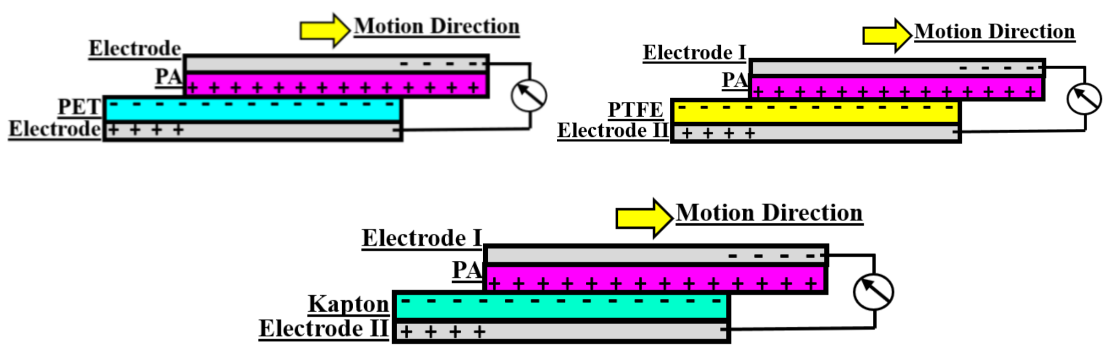

Fig. 1 The first sensor.

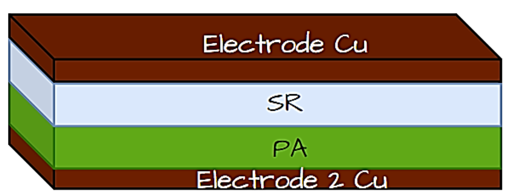

Fig. 2 The second sensor.

Fig. 3 The third sensor.

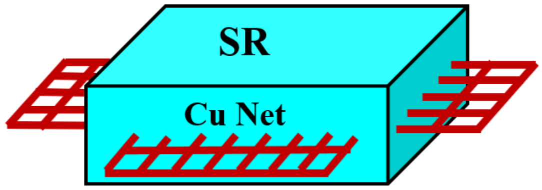

Fig. 4 The fourth sensor.

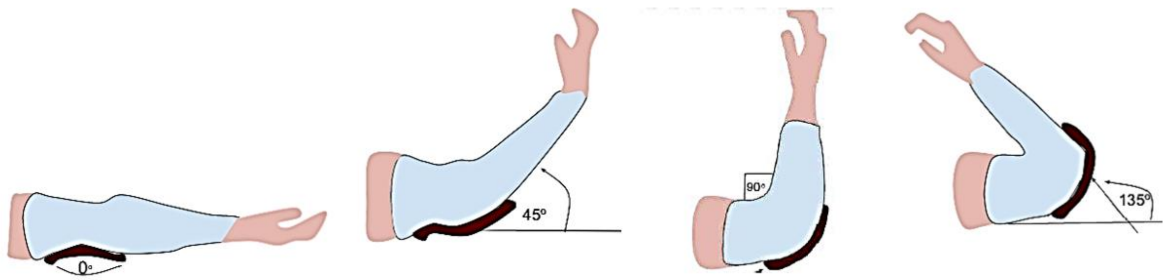

Fig. 5 Rotating angles of the arm.

RESULTS AND DISCUSSION

The output positive/negative voltage of the sensor as function of the rotating angle of the arm is shown in Figs. 6, 7, 8 and 9 for rotating angles of 45, 90, 135 and 180° respectively. The highest voltage values at 45° were +20 and -16 mV, Fig. 3. At 90°, the voltage values increased to +28 and -55 mV, Fig. 4. Increasing the angle to 135° caused voltage increase to +32 and -98 mV. While at 180° angle, voltage increased up to +56 and -158 mV. Figure 10 shows the relationship between output voltage of the sensor and the rotating angle. It is clearly seen that the proportionality is valid confirming the sustainability and suitability of the proposed sensor.

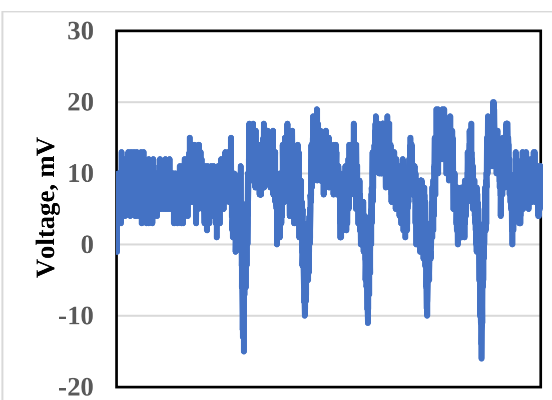

Fig. 6 Voltage generated from the rotation of the sensor 45°.

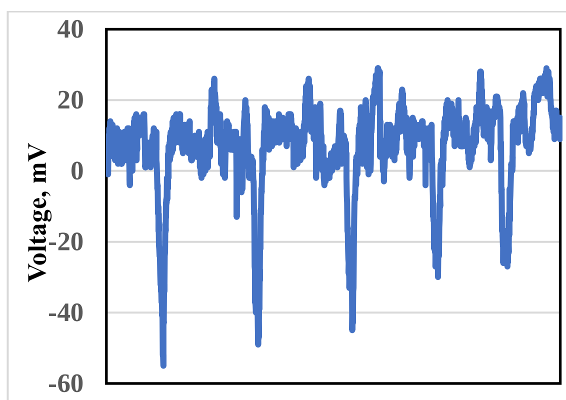

Fig. 7 Voltage generated from the rotation of the sensor 90°.

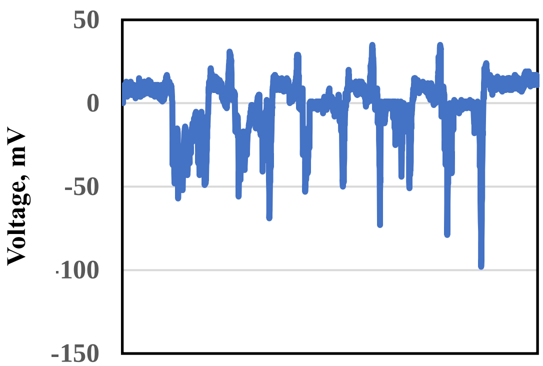

Fig. 8 Voltage generated from the rotation of the sensor 135°.

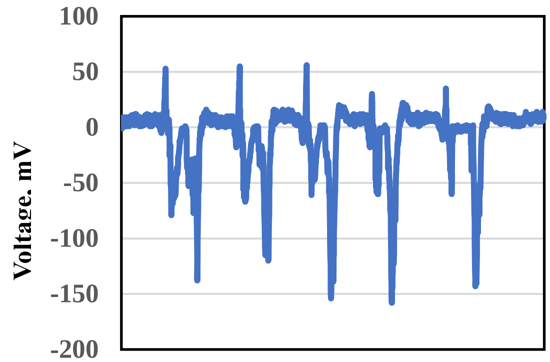

Fig. 9 Voltage generated from the rotation of the sensor 180°.

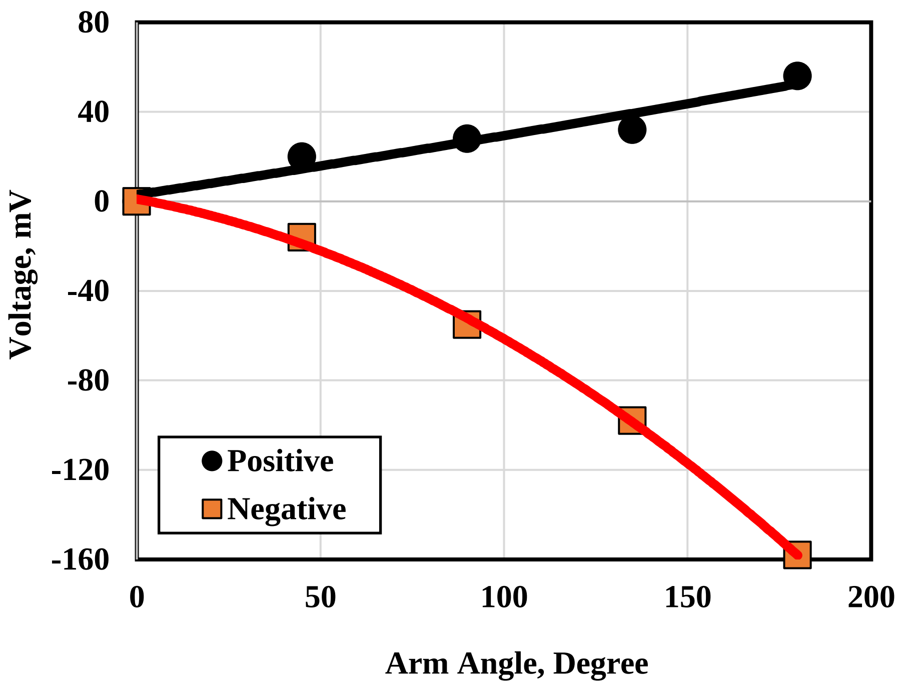

Fig. 8 The relationship between the generated voltage and the rotating angle of the sensor.

Figure 9 shows the voltage generated from the rotation of the sensor of different materials. Sensor consisted of PA and PTFE represented the highest values compared to PA/Kapton and PA/PET. That performance is due to the ranks of the tested surfaces in the triboelectric series. It is known that the gap between PA and PTFE is longer than the gap between PA and PET as well as PA and Kapton. Generally, as the angle of rotation increased, voltage significantly increased. This observation confirms the suitability of PA and PTFE for the design of the sensor.

Voltage generated from the rotation of the sensor consisting of thin and thick silicone rubber as negative friction surface contacting PA as the positive friction surface is illustrated in Fig. 10. It was reported that the silicone rubber is able to expand when stretched and contract during compression, [24, 25]. It is seen that thick SR displayed relatively higher voltage that thin one. The voltage values were relatively lower that that observed for PA/PTFE.

Figure 11 shows the relation between the generated voltage and the arm angle for sensor containing thin and thick SR reinforced by copper wire. The generated voltage was the result of the sliding of copper wire inside SR due to its super elastic property, where the stretch of the SR is much longer the deformation of the copper wire. Thick SR displayed higher voltage than thin SR, where the voltage value was 219 mV at 180° arm rotating angle.

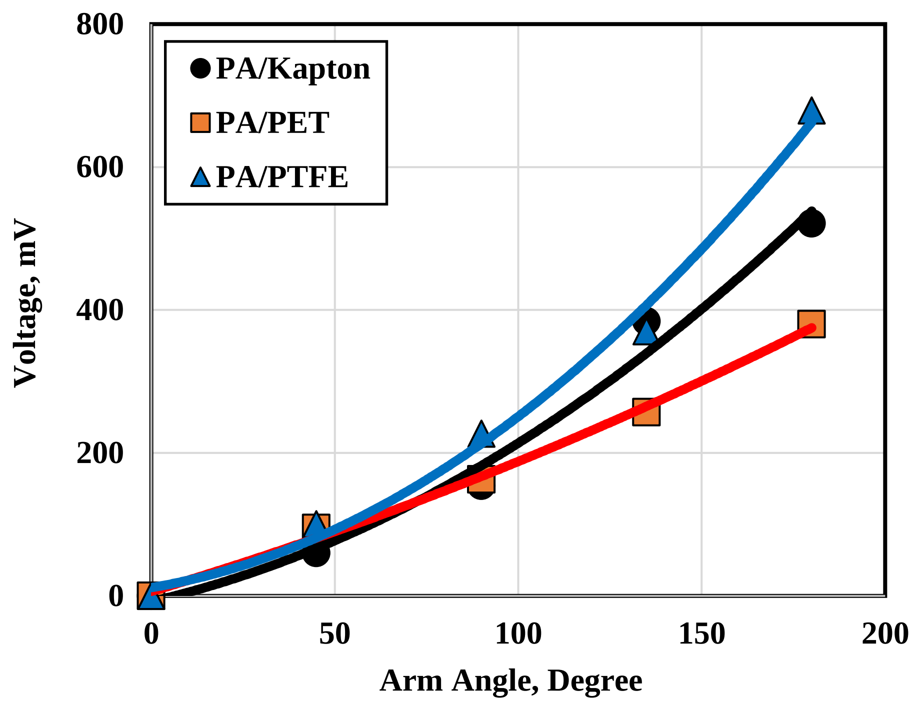

Fig. 9 Voltage generated from the rotation of the sensor of different materials.

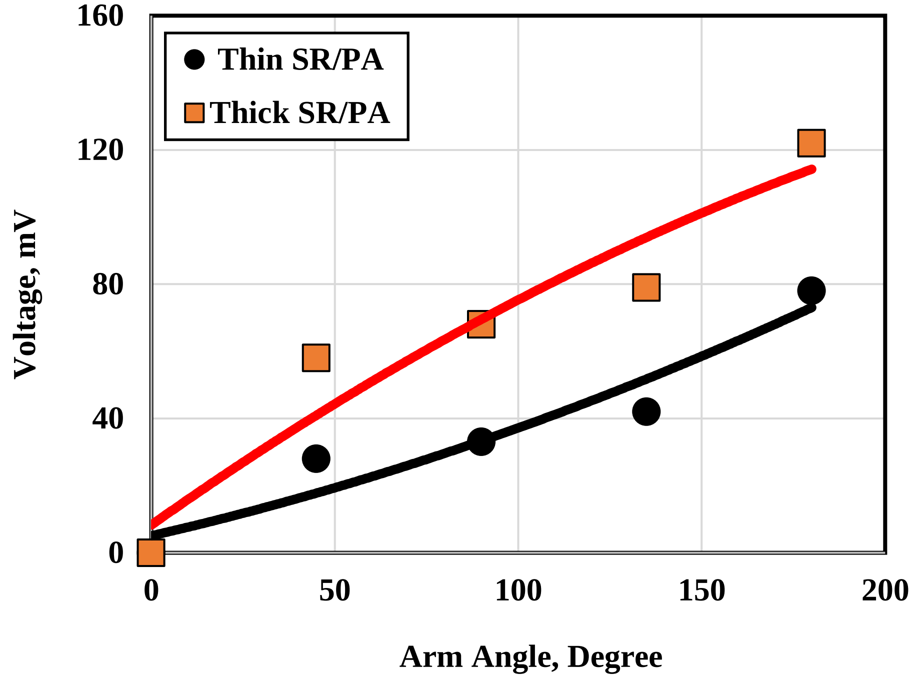

Fig. 10 Voltage generated from the rotation of the sensor consisting of thin and thick silicone rubber contacting polyamide.

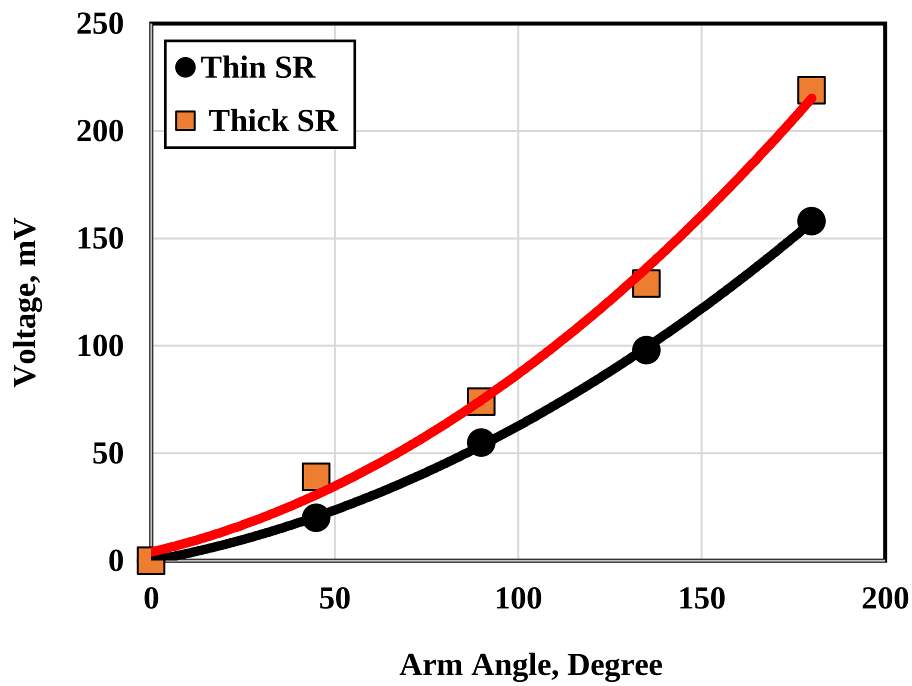

Fig. 11 Voltage generated from the rotation of the sensor consisting of thin and thick silicone rubber reinforced by copper wires.

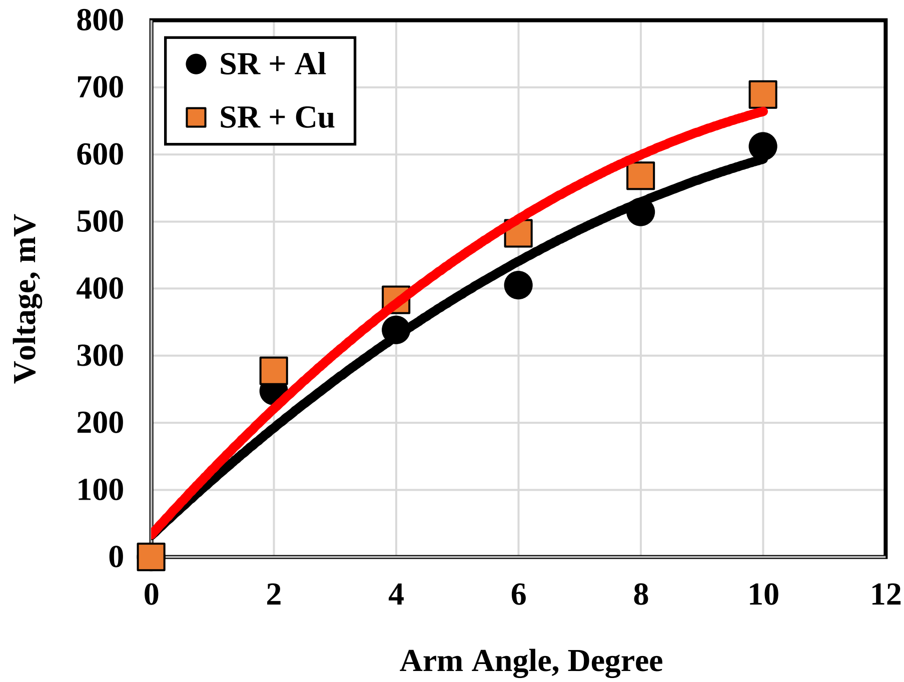

Fig. 12 Voltage generated from the rotation of the sensor consisting of thin silicone rubber reinforced by aluminum and copper nets.

Replacing the copper wire by Al and Cu nets reinforcing thin SR generated the highest voltage values up to 689 mV at 180° arm angle, Fig. 12. This is due to the increased surface area of the wires in the net. When the frictional surface of the copper wire contacts SR, the positive ESC generated on copper wire are equal to the negative one in the SR. During the slip of wire due to the difference in the stretch of SR and wire, the negative ESC generated on the SR transferred to ground, then reverse voltage could be measured from the wire terminal. This observation can be a motive for further experimental work to develop the design of the sensor.

CONCLUSIONS

1. The output voltage of the proposed sensor significantly increased with increasing the rotating angle of the arm.
2. Sliding PA on PTFE represented the highest values compared to PA/PET and PA/Kapton.
3. Thick SR displayed relatively higher voltage than that observed for thin one.
4. Reinforcing SR by Al and Cu nets reinforcing thin SR, generated the highest voltage values. Al and Cu nets recorded higher voltage than that measured for Cu wire because of the increased surface area of the wires in the net.

REFERENCES

1. Wu G., Li J., Xu Z., "Triboelectrostatic separation for granular plastic waste recycling: A review", Waste Management 33, pp. 585 - 597, (2013).
2. Matsusaka S., Maruyama H., Matsuyama T., Ghadiri M., "Triboelectric charging of powders: a review", Chem. Eng. Sci. 65, pp. 5781 - 5807, (2010).
3. Matsusaka S., Masuda H., "Electrostatics of particles" Adv. Powder Technol. 14, pp. 143 - 166, (2003).
4. Yoshida M., Ii N., Shimosaka A., Shirakawa Y., Hidaka J., "Experimental and theoretical approaches to charging behavior of polymer particles", Chem. Eng. Sci. 61, pp. 2239 - 2248, (2006).
5. Park C. H., Park J. K., Jeon H. S., Chun B. C., Triboelectric series and charging properties of plastics using the designed vertical-reciprocation charger", J. Electrostat, 66, pp. 578 - 583, (2008).
6. Meurig W. Williams, "Triboelectric charging in metal-polymer contacts - How to distinguish between electron and material transfer mechanisms", Journal of Electrostatics 71, pp. 53 - 54, (2013).
7. Sow M., Lacks D. J., Sankaran R. M., "Effects of material strain on triboelectric charging: Influence of material properties", Journal of Electrostatics 71 pp. 396 – 399, (2013).
8. Lee L. H., "Dual mechanism for metal–polymer contact electrification", J. Electrostat. 32, 1 - 29, (1994).
9. Matsusaka S., Masuda H., "Electrostatics of particles" Adv. Powder Technol. 14, pp. 143 - 166, (2003).
10. Blaise G., "Charge localization and transport in disordered dielectric materials", J. Electrostat. 50, pp. 69 - 89, (2001).
11. Pu X., Guo H., Tang Q., Chen J., Feng L., Liu G., Wang X., Xi Y., Hu C., Wang Z. L., "Rotation sensing and gesture control of a robot joint via triboelectric quantization sensor", Nano Energy 54, 453–460, (2018).
12. Li H., Zhang Y., Wu Y., Zhao H., Wang W., He X. and Zheng H., "A stretchable triboelectric nanogenerator made of silver-coated glass microspheres for human motion energy harvesting and self-powered sensing applications", Beilstein J. Nanotechnol., 12, 402–412, (2021).
13. Park J., Choi A. Y., Lee C. J., Kim D. and Y. T. Kim, "Highly stretchable fiber-based single-electrode triboelectric nanogenerator for wearable devices", The Royal Society of Chemistry, RSC Adv., , 7, 54829–54834, (2017).
14. Massoud M. A., Gehan A. M., Ali W. Y, and Abouelwafa W. A., "Revolutionizing Stroke Rehabilitation: Dynamic Glove-Based Rehabilitation System Empowered by CNN for Spastic Hands", IJT'2024, Vol.04, Issue 01, pp. 1 – 18, (2024).
15. Lindsay M. P. et al., "World Stroke Organization (WSO): Global Stroke Fact Sheet 2019," International Journal of Stroke, vol. 14, no. 8, pp. 806–817, Oct. (2019).
16. Lai S. M., Studenski S., Duncan P. W., and Perera S., "Persisting Consequences of Stroke Measured by the Stroke Impact Scale," Stroke, vol. 33, no. 7, pp. 1840–1844, Jul. (2002).
17. Bartels M. N., Duffy C. A. and Beland H. E., "Pathophysiology, Medical Management, and Acute Rehabilitation of Stroke Survivors," Stroke Rehabilitation. Elsevier, pp. 2 - 45, (2016).

18. Thibaut A., Chatelle C., Ziegler E., Bruno M.-A., Laureys S., and Gosseries O., "Spasticity after stroke: Physiology, assessment and treatment," Brain Inj, vol. 27, no. 10, pp. 1093 - 1105, (2013).
19. Venketasubramanian N., Yin A., Lee L. B., and De Silva D. A., "Two decades of nation-wide community-based stroke support – The Singapore National Stroke Association," International Journal of Stroke, vol. 12, no. 3, pp. 297 - 301, (2016).
20. Raghavan P., "Upper Limb Motor Impairment After Stroke," Phys Med Rehabil Clin N Am, vol. 26, no. 4, pp. 599 - 610, Nov. (2015).
21. Lance J. W., "What is spasticity?," The Lancet, vol. 335, no. 8689, p. 606, (1990).
22. Naro A.et al., "Breakthroughs in the spasticity management: Are non-pharmacological treatments the future?," Journal of Clinical Neuroscience, vol. 39, pp. 16 - 27, (2017).
23. Pitts D. G. and O'Brien S. P., "Splinting the Hand to Enhance Motor Control and Brain Plasticity," Top Stroke Rehabil, vol. 15, no. 5, pp. 456 - 467, (2008).
24. Ye X., He Y., Li S., Hu H., L. Gan, Huang J., "Auxetic wearable sensors based on flexible triboelectric polymers for movement monitoring", ACS Appl. Polym. Mater. 4, pp. 4339 - 4346, (2022).
25. Proto A., Penhaker M., Conforto S., Schmid M., "Nanogenerators for human body energy harvesting", Trends Biotechnol., 35, pp. 610 - 624, (2017).